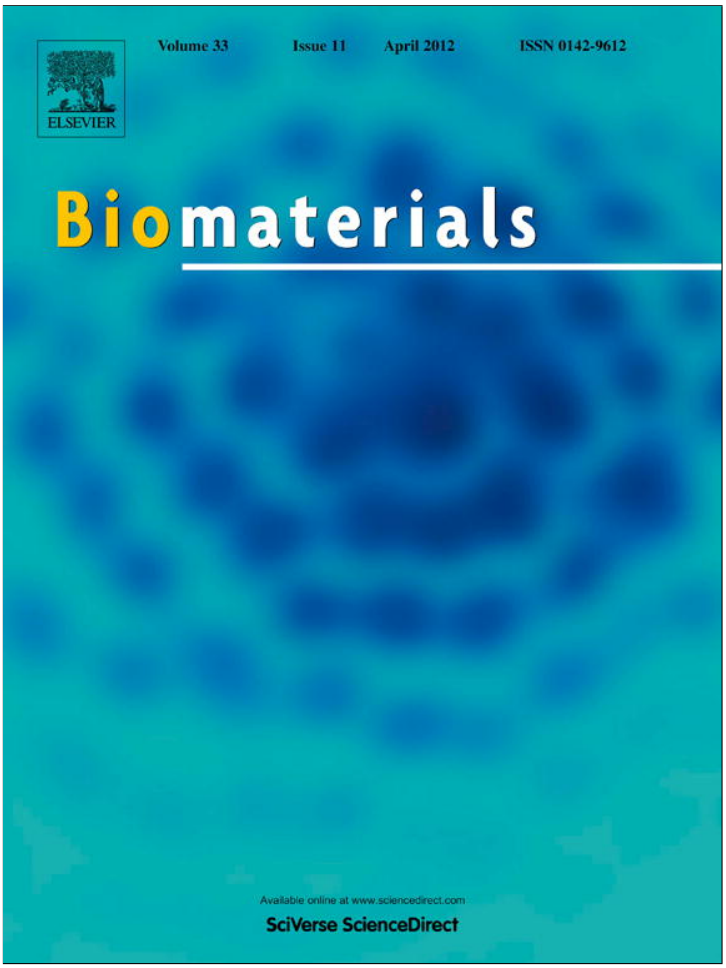

Biomaterials 33 (2012) 3243–3253

Contents lists available at SciVerse ScienceDirect

Biomaterials

journal homepage: www.elsevier.com/locate/biomaterials

Multi-arm polymeric nanocarrier as a nitric oxide delivery platform for chemotherapy of head and neck squamous cell carcinoma

Shaofeng Duan [1], Shuang Cai [1], Qiuhong Yang, M. Laird Forrest*

Department of Pharmaceutical Chemistry, The University of Kansas, 2095 Constant Ave, Lawrence, KS 66047, United States

ARTICLE INFO

Article history:
Received 14 November 2011
Accepted 9 January 2012
Available online 26 January 2012

Keywords:
Biocompatibility
Drug delivery
Drug release
Nanoparticle
Nitric oxide
Polymerization

ABSTRACT

Nitric oxide is a cell signaling molecule that can be a potent inducer of cell death in cancers at elevated concentrations. However, NO is also toxic to normal tissues and chronic exposure at low levels can induce tumor growth. We have designed a polymeric carrier system to deliver nitric oxide locoregionally to tumorigenic tissues at micromolar concentrations. A highly water solubility and biodegradable multi-arm polymer nanocarrier, sugar poly-(6-*O*-methacryloyl-D-galactose), was synthesized using MADIX/RAFT polymerization, and utilized to deliver high concentrations of nitric oxide to xenografts of human head and neck squamous cell carcinoma (HNSCC). The in vitro release of the newly synthesized nitric oxide donor, O^2-(2,4-dinitrophenyl) 1-[4-(2-hydroxy)ethyl]-3-methylpiperazin-1-yl]diazen-1-ium-1,2-diolate and its corresponding multi-arm polymer-based nanoconjugate demonstrated a 1- and 2.3-fold increase in half-life, respectively, compared to the release half-life of the nitric oxide-donor prodrug JS-K. When administered to tumor-bearing nude mice, the subcutaneously injected multi-arm polymer nitric oxide nanoparticles resulted in 50% tumor inhibition and a 7-week extension of the average survival time, compared to intravenous JS-K therapy. In summary, we have developed an effective nitric oxide anti-cancer chemotherapy that could be administered regionally to provide the local disease control, improving prognosis for head and neck cancers.

1. Introduction

The clinical outcomes and overall survival rates for advanced HNSCC have not improved significantly over the past two decades despite advancements in surgery and treatment, so that HNSCC continues to affect over a half million new patients worldwide each year [1]. Moreover, the current therapies for head and neck cancer result in numerous adverse effects, some permanent such as possible loss the salivary gland function and muscle control in the shoulders. Thus, there is a clear need for less damaging therapies for head and neck cancer that will achieve a more favorable clinical outcome and reduce treatment morbidity [2].

Nitric oxide is a cell signaling molecule involved in many mammalian physiological processes and pathological conditions. The effects of nitric oxide on tissues are highly concentration dependent. Low levels of nitric oxide synthase (NOS) over-expression in cancer cells is frequently associated with enhanced tumor cell invasion and growth [3,4] and an increase in aerobic glycolysis capacity [5], i.e. the Warburg effect. However, high concentrations of nitric oxide can inhibit NF-kB activity, which regulates cell proliferation, and downregulating Bcl-xL expression, which modulates apoptotic pathways [6,7]. Nitric oxide has been shown to radiosensitize cancers, inhibit DNA repair mechanisms, inhibit hypoxia-induced drug resistance, and reverse the epithelia to mesenchyma phenotype transition of tumors [8–10]. Nitric oxide has a half-life of about 5 s in vivo, due to rapid reaction of the unpaired electron with hemoglobin and heme ferrous iron and subsequent decomposition into nitrate [11]. Therefore, nitric oxide donating prodrugs have been developed for anti-cancer therapy, such as JS-K [12]. JS-K is a GST-activated nitric oxide prodrug, releasing nitric oxide in vitro, inhibiting the proliferation of cancer cells, including breast cancer cells [13], non-small-cell lung cancer cells [14] and myeloma cells [15]. Because GSTs are also expressed in normal mammalian organs [16], the potential toxicity and carcinogenicity of JS-K must not be overlooked.

The potential for dose-dependent carcinogenicity of nitric oxide-releasing agents has limited their development as systemically administered anti-cancer agents. The effective and safe use of these agents requires that the nitric oxide release be highly confined to tumorigenic tissues and exposure to sub-therapeutic doses must be minimized. The tissue distribution of

* Corresponding author. Tel.: +1 785 864 4388; fax: +1 785 864 5736.
E-mail address: mforrest@ku.edu (M.L. Forrest).
[1] Both authors contributed equally to this work.

0142-9612/$ – see front matter © 2012 Elsevier Ltd. All rights reserved.
doi:10.1016/j.biomaterials.2012.01.026

small molecule drugs is typically non-specific, with increased exposure in clearance organs, such as the kidneys and liver. To overcome this challenge, a drug molecule may be conjugated to a targeted delivery system so that it will be preferentially released in tumorigenic cells. Water-soluble polymers have been utilized for the preparation of drug conjugates that display significant advantages in pharmaceutical applications, including low toxicity, excellent water solubility, and tissue targeting through passive (e.g. enhanced permeation and retention effect) or receptor-based targeting [17]. Despite the targeted nature of these carriers in intravenous applications, healthy tissues will still receive substantial exposure due to long residence in the clearance organs and circulatory system. Our group and others have partially overcome this problem by delivering nanoconjugates directly to the primary tumor and the draining lymphatics [18–25]. This approach can greatly improve the response in locally advanced cancers, since the nanoconjugate and method of administration can confine the drug to only the tumor and the lymph nodes draining the tumor. An issue in the design of these drug delivery systems is the carrier must be very stable within the extravascular space, which limits the use of micelles and liposomes, and it should be under 50 nm in size for rapid clearance from the injection site. Structured polymers such as dendrimers meet these requirements [26–29], but dendrimers such as PAMAM constructs are not biodegradable and have limited capacity for water-insoluble drugs. Multi-arm or star polymers are branched nanoscale materials that have a compact structure, globular shape, and large surface area that make them highly suited for targeted drug delivery when built with non-toxic and biodegradable polymers.

Multi-arm polymers can be synthesized under a broad range of conditions with low polydispersity using reversible addition-fragmentation chain transfer polymerization (RAFT). During the RAFT process, the polymers derived keep their “livingness” so that it is possible to prepare well defined polymers. Moreover, The RAFT process is tolerant toward a range of functional groups thus minimizing the need for additional synthetic pathways to install protecting groups on the monomers being used. In this study, we report the synthesis of a 4-arm sugar-decorated polymer (Fig. 1) using MADIX/RAFT polymerization and two nitric oxide-releasing analogues based on JS-K.

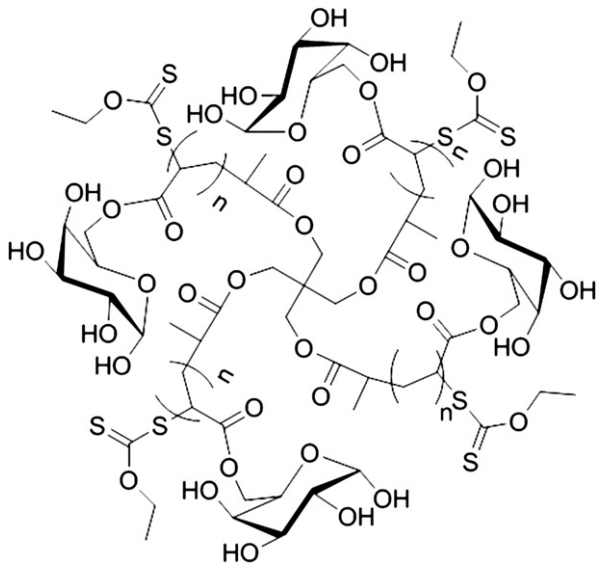

Fig. 1. Structure of a multi-arm sugar polymer.

2. Materials and methods

2.1. Materials

Unless noted otherwise, all reagents and solvents were purchased from Sigma Aldrich and used without further purification. ^{1}H-NMR (400 MH_z) and ^{13}C-NMR (100 MH_z) spectra were collected on a Bruker DRX 400 spectrometer using compounds dissolved in $CDCl_3$, MeOD or D_2O. Chemical shifts were referenced to δ7.28 and 77.0 ppm for ^{1}H-NMR and ^{13}C-NMR spectra, respectively. High-resolution mass spectrometry (HRMS) data were generated after flow injection analysis (FIA) by manually matching peaks on an Applied Biosystems Mariner TOF spectrometer with a turbo-ionspray source. The Griess Reagent kit was purchased from Promega Corporation (Madison, WI). Cell culture media were purchased from Fisher Scientific (Pittsburgh, PA).

2.2. Synthesis

2.2.1. Synthesis of MADIX/RAFT agent

The MADIX/RAFT agent was synthesized based on the procedure reported previously (Fig. 2) [30]. Pentaerythritol was used as the starting material to react with 2-bromopropionyl bromide and *O*-ethylxanthic acid (potassium salt) successively to form a four-arm sulfur compound which was used as the MADIX/RAFT initiator agent.

2.2.1.1. Reaction of the 4-arm core with 2-bromopropionyl bromide. Pentaerithol (1.36 g, 10 mmol) was dissolved in 25 mL of dry chloroform and 2.5 mL of pyridine and cooled to 0 °C. The 2-bromopropionyl bromide (10.01 g, 45 mmol) was added dropwise, and the reaction proceeded at ambient temperature (ca. 23 °C) for 48 h. The mixture then was neuralized with aqueous HCl (10 wt%). Then the organic phases were washed with water, sodium bicarbonate solution (5%) and brine, followed by drying with sodium sulfate. Evaporation of the solvent under reduced pressure yielded the desired compound, and the molecular structure was verified by ^{1}H-NMR and compared with the reported data.

2.2.1.2. Reaction of bromide intermediate with O-ethylxanthic acid (potassium salt). A solution of the intermediate compound (2.028 g, 3.0 mmol) in chloroform (45 mL) was treated with a 10-fold excess of O-ethylxanthic acid, potassium salt (5.01 g, 30 mmol). The mixture was stirred at ambient temperature for 3 days, and the resulting suspension was filtered and washed with chloroform. Evaporation of the solvent followed by purification through a flash column on silica gel using 3:7 ethyl acetate:hexanes as eluents yielded the desired compound, and the molecular structure was verified by ^{1}H-NMR and compared with the reported data.

2.2.1.3. Synthesis of 1,2;3,4-di-O-isopropylidene-6-O-acryloyl-α-d-galactopyranose (AlpGP). The RAFT agent was synthesized according to the procedure of Ting et al. [31]. Briefly, to a 100 mL round bottom flask were added *1,2,3,4-di-O*-isopropylidene-*6-O*-acryloyl-*α-d*-galactopyranose (1.39 g, 5.20 mmol), basic alumina (2.44 g, 23.92 mmol), 20 mL of dry acetonitrile, and acryloyl chloride (2.26 mL, 27.04 mmol), dropwise. After stirring under argon for 3 days at ambient temperature, the mixture was filtered through a thin layer of celite, and the solids were washed with 50 mL of acetonitrile. The combined organic layers were concentrated under reduced pressure. The resulting pale yellow residue was purified through a flash column using 1:2 ethyl acetate:hexanes as eluents, and its molecular structure was verified by ^{1}H-NMR and compared with the reported data.

2.2.2. Synthesis of a multi-arm sugar polymer

2.2.2.1. Synthesis of poly-(1,2:3,4-di-O-isopropylidene-6-O-methacryloyl-α-D-galactopyranose) with the MADIX/RAFT agent. The *1,2,3,4-di-O*-isopropylidene-*6-O*-acryloyl-*α-d*-galactopyranose (3.11 g, 9.9 mmol) was treated with basic alumina and 10 mL of dry α, α, α- trifluorotoluene in a 50 mL round bottle flask. The RAFT agent (0.054 g, 0.0622 mmol) was added to the solution, followed by the addition of AIBN (1.36 mg, 0.00827 mmol), and the reaction flask was placed on ice and purged with argon for 30 min. The flask was then transferred to a thermostatic oil bath at 70 °C for ca. 10 h. The mixture was cooled in an ice bath and poured into cold diethyl ether to obtain the precipitate followed by concentration under reduced pressure (Fig. 2). The molecular structure and molecular weight of the resulting polymer were determined by ^{1}H-NMR and size exclusion chromatography (SEC), respectively.

2.2.2.2. Synthesis of multi-arm poly-(6-O-methacryloyl-D-galactose). The poly-(*1,2:3,4-di-O*-isopropylidene-*6-O*-methacryloyl-α-D-galactopyranose) (500 mg) was dissolved in 100 mL of 90% formic acid. The solution was stirred at 60 °C for 24 h. The solution then was dialyzed (10 kDa tubing, Pierce, Rockford, IL) against distilled water for 2 days with water changes every 6 h to remove the acid. After dialysis, the resulting polymer was lyophilized to obtain the desired multi-arm poly-(*6-O*-methacryloyl-D-galactose) (Fig. 2).

2.2.3. Modification of multi-arm poly-(6-O-methacryloyl-D-galactose) with succinic anhydride

Polymers with increasing degree of succination (20%, 40%, 60% and 90%) were generated by reacting the star poly-(*6-O*-methacryloyl-D-galactose) (100 mg) with

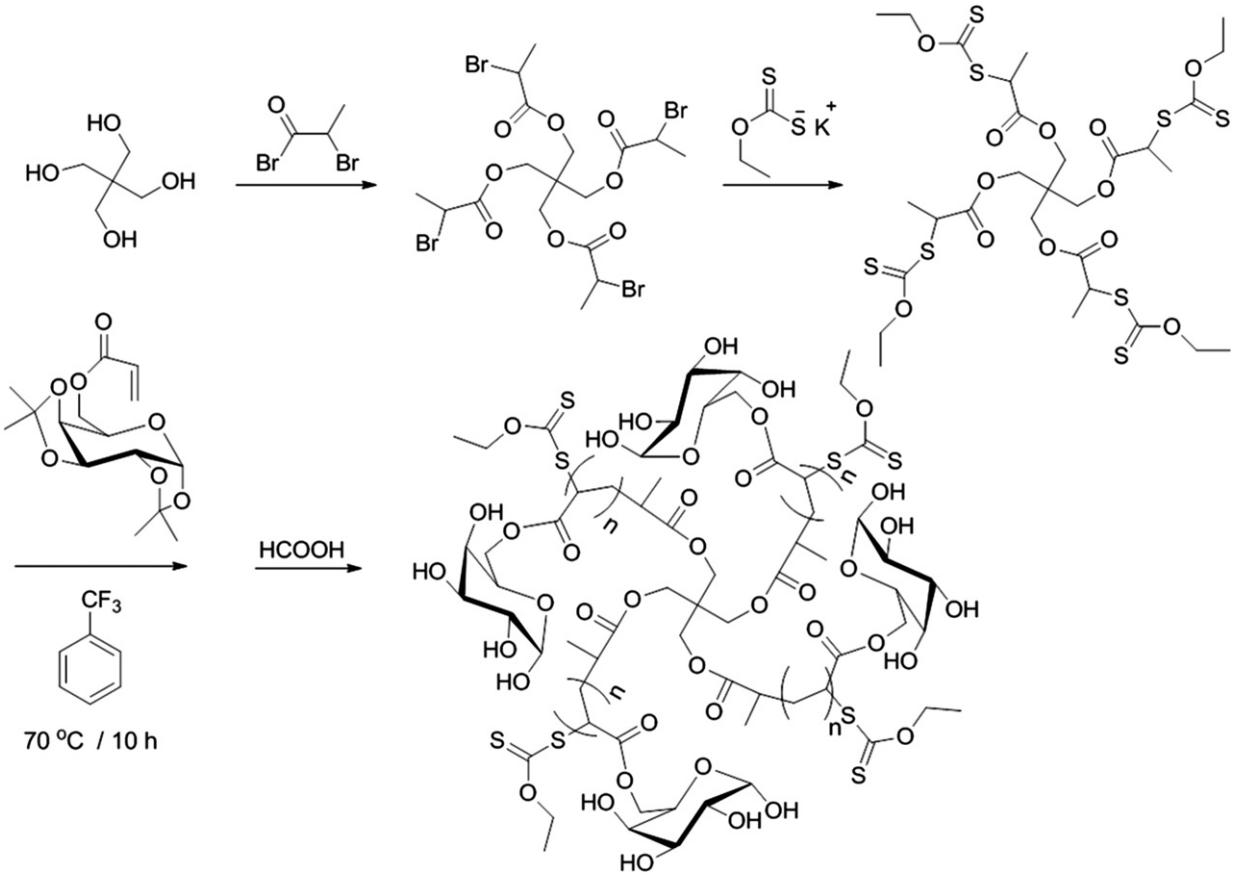

Fig. 2. Synthesis of a multi-arm poly-(6-*O*-methacryloyl-D-galactose).

succinic anhydride (20, 40, 60 and 90 mg, respectively) in 20 mL of dry dimethyl formaldehyde (Fig. 3). The mixtures were stirred at ambient temperature to form a homogeneous solution, followed by dropwise addition of 5 mL of dry pyridine. After 2 days, the solutions were dialyzed (10 kDa tubing) against 50% ethanoic water for 1 day followed by absolute ethanol for 1 day, with solvent changes every 6 h to remove the dimethyl formaldehyde, pyridine, and other small molecule impurities. Lyophilization of the resulting solution led to the desired sugar multi-arm polymers with increasing substitution degrees of carboxylic acids.

2.2.4. Synthesis of JS-K and JS-K analogues

The nitric oxide-donating prodrug JS-K, O^2-(2, 4-Dinitrophenyl) 1-[(4-ethoxycarbonyl) piperazin-1-yl] diazen-1ium-1, 2-diolate was synthesized. The

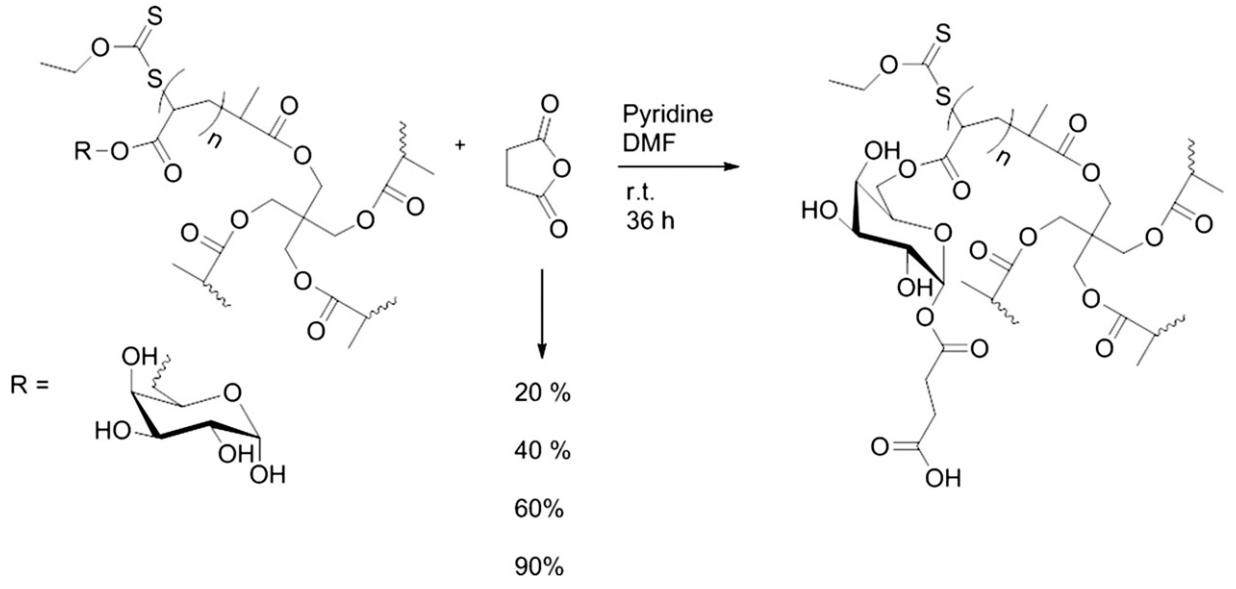

Fig. 3. Modification of multi-arm poly-(6-*O*-methacryloyl-D-galactose) with succinic anhydride resulted in polymers with increasing degree of acid substitution (20, 40, 60 and 90% wt/wt).

synthetic route is depicted in Fig. 4. Briefly, to a 250 mL round bottom flask were added 2.10 g of compound 1 (5.09 mmol) and 130 mL of ethyl acetate. After the mixture was cooled to 0 °C, 11.5 mL of concentrated HCl was added dropwise. The reaction was allowed to warm to ambient temperature and stirred overnight. The resulting suspension was filtered and the yellow solid was washed with 100 mL of ethyl acetate and then dried under reduced pressure. The desired compound 2 was obtained without further purification, and the molecular structure was verified by ^{1}H-NMR, ^{13}C-NMR and high resolution mass spectrometry (HRMS).

Subsequently, compound 2 (0.132 g, 0.38 mmol) and ethyl chloroformate (56 μL, 0.57 mmol) were combined in 4 mL of dry THF. After cooling to 0 °C, triethylamine (1.14 mmol) was added. The reaction was kept at 0 °C for 10 min and then stirred at ambient temperature for 3 h or until TLC indicated complete consumption of compound 2. The mixture was diluted with 10 mL of THF, and the organic phase was washed with water, saturated sodium bicarbonate solution and brine, and dried over sodium sulfate. Evaporation of the solvent under reduced pressure followed by purification of the residue using silica gel flash chromatography with 1:1 ethyl acetate:hexanes as eluents led to the desired compound JS-K (compound 3), and the molecular structure was verified by ^{1}H-NMR, ^{13}C-NMR and HRMS.

2.2.4.1. Synthesis of JS-K analogue 2,O^{2}-(2,4-dinitrophenyl) 1-[[4-(2-hydroxy)ethyl]-3-methylpiperazin-1-yl]diazen-1-ium-1,2-diolate. The JS-K analogue NO2 (compound 4) was synthesized according to Chakrapani's procedure with modifications [32] (Fig. 5). Briefly, a solution of 1-(butyloxycarbonyl) homopiperazine (10 g, 50 mmol) in methanol (2 mL) was treated with 25% w/v methanolic sodium methoxide (9.3 mL) and ether (10 mL). The resulting solution was charged with 60 psi NO and stirred at ambient temperature for 24 h. A white precipitate was filtered, washed with ether, and dried under reduced pressure to afford sodium 1-[(4-*tert*-butoxycarbonyl) homopiperazin-1-yl] diazen-1-ium-1, 2-diolate, and the molecular structure was verified by ^{1}H-NMR, ^{13}C-NMR and HRMS.

2.2.4.2. Synthesis of JS-K analogue 1,O^{2}-(2,4-dinitrophenyl) 1-{[4-(2-(2-hydroxyethoxy)) ethyl] piperazin-1-yl}diazen-1-ium-1,2-diolate. The JS-K analogue NO1 (compound 5) was synthesized based on the synthesis of analogue 2 using 1-[2-(2-hydroxyethoxy) ethyl] piperazine (5.0 g, 27.3 mmol) as the starting material (Fig. 5). The resulting crude compound was purified through chromatography on silica gel using 1:1 ethyl acetate:hexanes as eluents to afford the desired compound, and the molecular structure was verified by ^{1}H-NMR, ^{13}C-NMR and HRMS.

2.2.5. Synthesis of multi-arm poly-(6-O-methacryloyl-D-galactose)-acid-NO 1 conjugate (multi-arm polymer-JSK analogue 1 conjugate)

Multi-arm poly-(6-*O*-methacryloyl-D-galactose)-60% (50 mg) was dissolved in 25 mL of DMF: dd H_2O (25:1 v/v). After a homogeneous solution formed, EDCI·HCl (1.5 eq) and HOBt·H_2O (1.5 eq) were added and the temperature was kept at 0 °C. After 5 min, JS-K analogue NO1 (1.0 eq) was added. The reaction proceeded at 0 °C for 30 min and then at ambient temperature overnight under argon. The resulting solution was dialyzed against 50% v/v ethanol in water for 12 h and then absolute ethanol for 12 h using 10 kDa dialysis tubing (Fig. 6). Removal of the solvent under reduced pressure led to the desired conjugate, and the molecular structure and drug loading degree were determined by ^{1}H-NMR.

2.3. Characterization

2.3.1. Size exclusion chromatography

The molecular weights and polydispersity indices (PDIs) of the multi-arm polymers *d,l-PLA-block-PAIpGP* were determined using EZStart 7.4 software and a Shimadzu 2010CHT system equipped with an RID-10A refractive index detector and a TSK gel multipore Hx-M 7.8 × 30 cm column. The mobile phase contained 10 mM LiCl in DMF (0.8 mL/min). The calibration curve was generated using polystyrene standards ranging from 1180 to 339,500 g/mol. After deprotection, the resulting multi-arm poly-(6-*O*-methacryloyl-D-galactose) was highly soluble in methanol, water, DMF, and DMSO. The molecular weights of the acid multi-arm polymers were determined by SEC using the same condition except that the system was calibrated using polyethylene glycol (PEG) standards ranging from 3070 to 66,100 g/mol (Scientific Polymer Products, Inc). The degree of substitution was determined by ^{1}H-NMR in MeOD, based on the ratio of the methylene protons of the acid groups to the protons of the sugar groups.

2.3.2. NMR

The molecular structures of the MADIX/RAFT agent, 4-arm polymer, acid derivatives of the 4-arm polymers, JS-K and its analogues (NO1 and NO2), and the 4-arm polymer-NO1 conjugates (sugar-NO1) were determined by ^{1}H-NMR, ^{13}C-NMR and HRMS. The substitution degrees of the acid groups on the sugar multi-arm polymer were determined by ^{1}H-NMR based on the ratio of the methylene protons of the acid groups to the protons of the sugar groups. The following sugar acid polymers have been made successfully: sugar-20% acid, sugar-40% acid, sugar-60% acid, sugar-90% acid. In addition, the substitution degree of NO1 prodrug on the sugar-NO1 conjugate was also determined by ^{1}H-NMR.

2.3.3. Solubility

The water solubilities of multi-arm poly-(6-*O*-methacryloyl-D-galactose) and its acid-modified derivatives were measured in 1× PBS (pH 7.4) at 37 °C. The solutions were kept under this condition and monitored for precipitation for 24 h.

2.3.4. Viscosity

The viscosity parameters were measured using a Stabinger viscometer (SVM 3000, Anton Paar, USA). A series of sugar multi-arm polymer samples with or without acid modification (20%, 40%, 60% and 90% wt/wt) were prepared by dissolving the polymers in ddH_2O at three concentrations including: 1.0 mg/mL, 3.0 mg/mL and 10.0 mg/mL. The viscosity measurements are reported in Table 1.

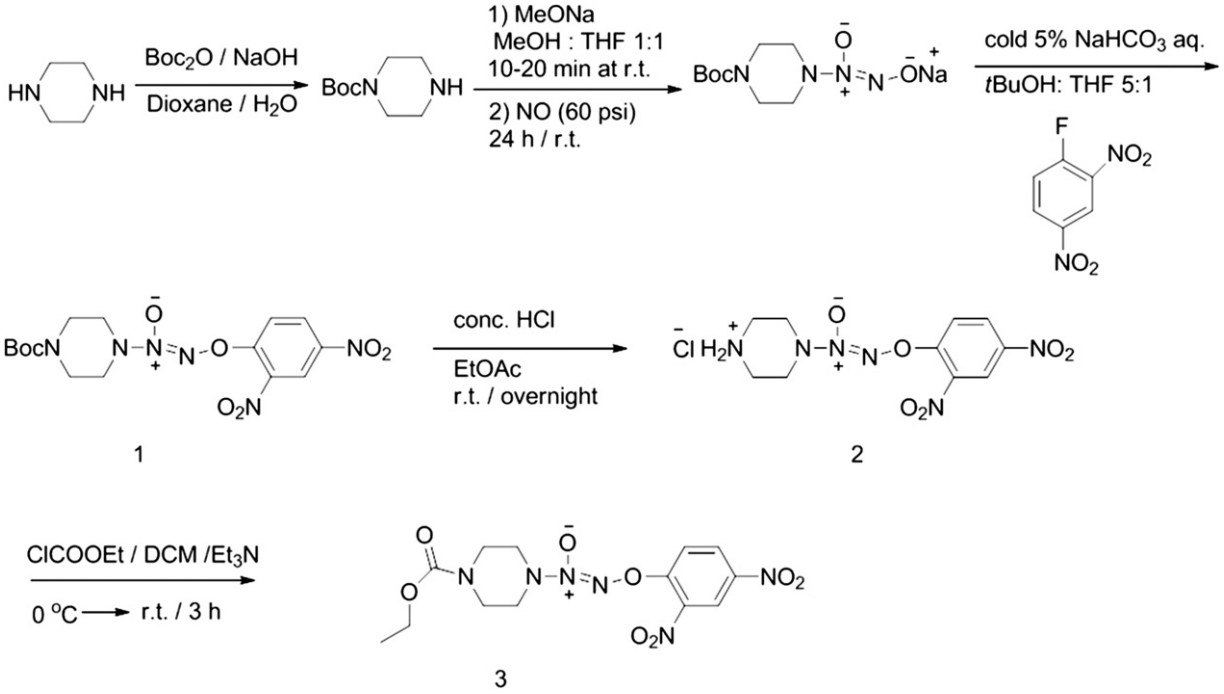

Fig. 4. Synthesis of JS-K.

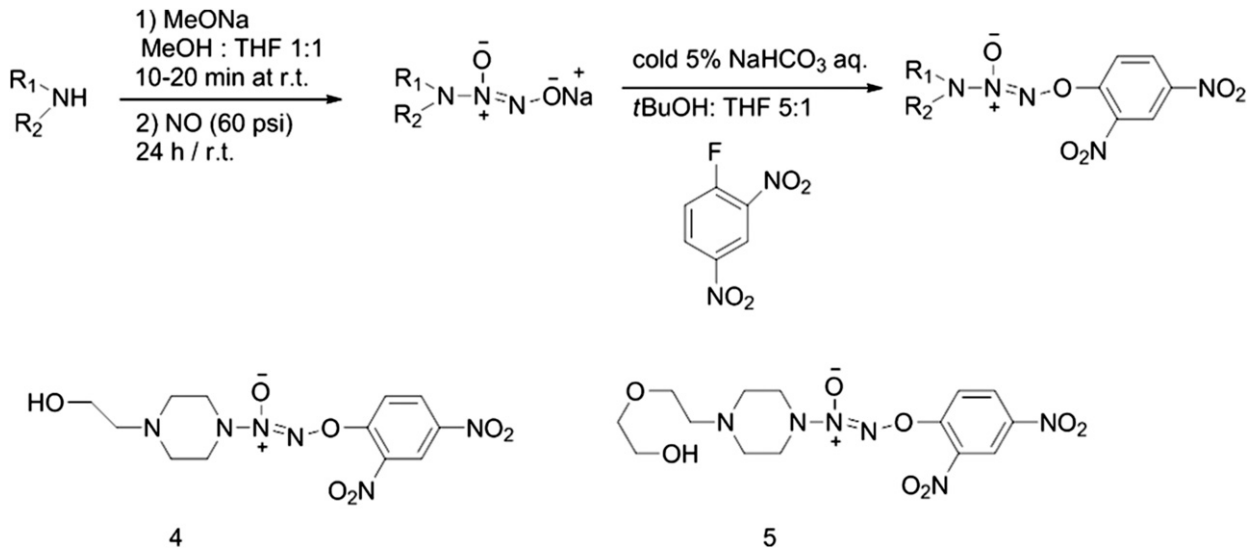

Fig. 5. Synthesis of JS-K analogues.

2.4. Cytotoxicity

Cell growth inhibition was determined in 96-well plates (3000 cells/well in 100 μL, 12 replicates/sample) using highly invasive human breast cancer cells, MDA-MB-231, non-metastatic human breast cancer cells, MDA-MB-468, and highly invasive human head and neck squamous cell cancer cells positive for epithelia growth factor receptor, MDA-1986. Drug or conjugate solutions were applied after 24 h, and 72 h post-addition, resazurin blue in 10 μL of PBS was applied to each well (final concentration 5 μM). After 4 h, well fluorescence was measured (ex/em 560/590) (SpectraMax Gemini, Molecular Devices), and the IC_{50} concentration determined as the midpoint between drug-free medium (positive) and cell-free (negative) controls.

2.5. Nitric oxide release

To determine the release half-life of nitric oxide from JS-K, NO1, NO2 and sugar-NO1, MDA-1986 cells were seeded in 96-well plates 24 h prior to drug treatment (100 μL/well). On the following day, cells were treated with 20 μM of either one of the nitric oxide prodrugs (NO1, NO2 or JS-K) or the polymer-based sugar-NO1. Fifty microliters of cell culture media were collected from each plate at 10 min, 2, 7, 22, 48 and 96 h, post treatment to determine the nitrite content ($N = 5$). The Griess reaction was performed according to the manufacturer's protocol. The fluorescence intensity was measured between 520 and 550 nm using a fluorescence microplate reader. The nitrite concentration and the corresponding nitrite oxide levels were determined using the nitrite standard curve previously generated.

2.6. Tumor model and efficacy

The MDA-1986 human head and neck squamous cell carcinoma cells were prepared in PBS at a concentration of 2×10^7 cells/mL. Female nude mice were anesthetized with 1.5% isoflurane in 50% O_2:air mixture, and 50 μL of cell solution was injected into the sub-mucosa of the mice using a 30-ga needle.

This xenograft model has been used in our laboratory to evaluate a hyaluronan-based drug delivery system [19]. The tumor cells were implanted at the same time for all groups of animals. The treatments began once the primary tumors reached 50–100 mm^3, which typically occurred within 2 weeks of implantation. The tumor growth was monitored 2–3 times weekly by measurement with a digital caliper in two perpendicular dimensions, and the tumor volume was calculated using the equation: tumor volume $= 0.52 \times (\text{width})^2 \times (\text{length})$. Animals were euthanized when their tumor size reached 1000 mm^3 or the body score index dropped below 2 [33].

Animals bearing head and neck tumors were randomly divided into 3 groups, including Sugar-NO1 s.c. group ($N = 11$), JS-K i.v. group ($N = 7$) and untreated control group ($N = 8$). The treatments were administered subcutaneously next to the tumor two week after tumor cell implantation, at a dose of 10 mg/kg on the basis of NO prodrugs.

Table 1
Molecular weights, PDIs and viscosities of acid derivatives of sugar multi-arm polymer.

Acid%	M_{theo}, g/mol	M_n, GPC[a], g/mol	PDI	Viscosity$_{1\ mg/mL}$, $mm^2\ s^{-1}$	Viscosity$_{10\ mg/mL}$, $mm^2\ s^{-1}$
0	54,610	45,460	1.20	1.0557	1.0808
20	54,610	45,890	1.19	1.0473	1.1131
40	63,640	54,390	1.17	1.0488	1.1017
60	72,730	60,110	1.21	1.0451	1.0952
90	86,370	75,100	1.15	1.0536	1.1033

[a] Standard: PEG; mobile phase: DMF (10 mM LiCl); flow rate: 0.8 mL/min.

3. Results

3.1. Synthesis

The yield of the MADIX/RAFT polymerization reaction mediated by xanthates was ca. 90%. The NMR results demonstrated that the satisfactory conversion and polymerization were obtained when the reaction was allowed to proceed for 8–12 h. After deprotection, the resulting sugar multi-arm polymer is highly soluble in water and organic solvents, including MEOH, $EtOH_3$, DMF and DMSO. The sugar multi-arm polymers were further modified using succinic anhydride to yield multi-arm polymers with increasing degrees (20, 40, 60 and 90%) of terminal carboxylic acid groups on the polymer arms.

The nitric oxide prodrug JS-K and its two analogues were successfully synthesized; the yields of the reactions are reported in NMR 3.3.2. The analogue number 1, O^2-(2,4-dinitrophenyl) 1-[4-(2-hydroxy)ethyl]-3-methylpiperazin-1-yl]diazen-1-ium-1,2-diolate, was selected to be further conjugated onto the sugar multi-arm polymer with 60% acid substitution, resulting in the formation of a multi-arm polymer-NO1 conjugate. The substitution degree of NO1 prodrug on the conjugate was determined to be approximately 12% (wt/wt) based on the ratio of the aromatic protons of the NO1 prodrug to the protons of the repeating units of the multi-arm polymer backbone.

3.2. Characterization

3.2.1. Size exclusion chromatography

The molecular weight of the multi-arm poly-(*1,2:3,4-di-O*-isopropylidene-6-*O*-methacryloyl-α-D-galactopyranose) synthesized was determined by SEC using polystyrene polymers as standards.

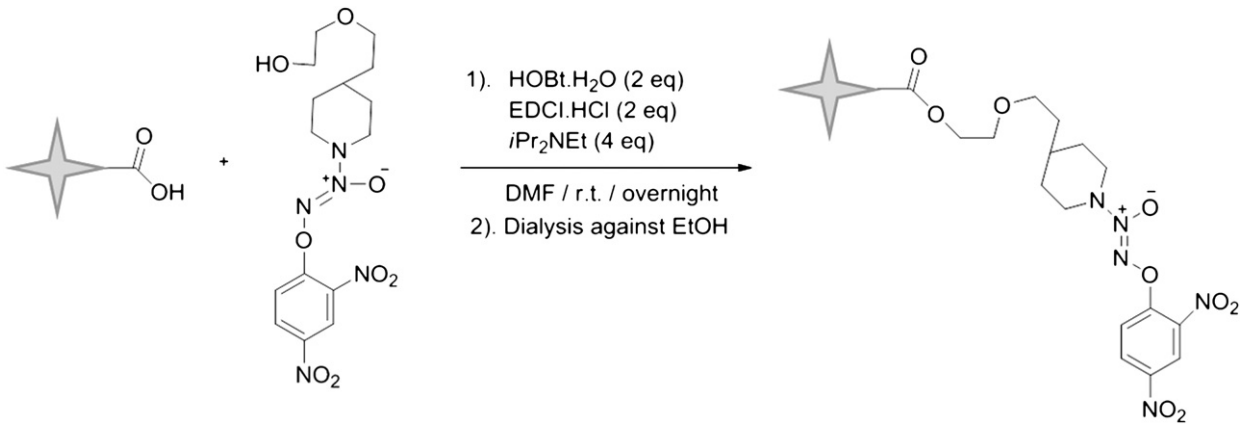

Fig. 6. Synthesis of acid sugar multi-arm polymer-JS-K analogue NO1 conjugate (sugar-NO1).

The number average molecular weight, M_n, and the polydispersity index, PDI, were determined to be 73,292 g/mol and 1.13, respectively (Fig. 7). After the removal of the isopropylidene protecting groups within the multi-arm polymer, the molecular weight of the resulting multi-arm poly-(6-*O*-methacryloyl-D-galactose) was determined by SEC under the same condition except that PEG polymers were used as standards. The M_n and PDI were determined to be 45,460 g/mol and 1.20, respectively (Fig. 7). After the modification of the multi-arm poly-(6-*O*-methacryloyl-D-galactose) with succinic anhydride, the resulting acid derivatives of the polymer were analyzed by SEC and their molecular weights and PDIs are reported in Table 1.

3.2.2. NMR

The molecular structures of JS-K and its two analogues were determined by ^{1}H-NMR, ^{13}C-NMR and HRMS. The substitution degrees of the carboxylic acid groups on the arms of the sugar multi-arm polymer were determined by ^{1}H-NMR for all four acid derivatives of the polymer, based on the ratios of the methylene protons of the acid groups to the protons of the sugar side chains. In addition, the substitution degree of NO1 on the sugar multi-arm polymer backbone was also determined by ^{1}H-NMR. The chemical shifts of all NMR spectra were measured as follows.

3.2.2.1. Synthesis of MADIX/RAFT agent. The desired bromo intermediate was obtained with a yield of 72% (4.89 g). ^{1}H-NMR ($CDCl_3$, 400 MHz) δ: 1.85 (d, 12 H, $J = 7.0$), 4.22–4.23 (m, 4H), 4.33–4.39 (m, 4H), 4.41 (q, 4 H, $J = 7.0$). The chemical shifts are consistent with the structure and no impurities or unknown peaks were observed.

The desired MADIX/RAFT compound was obtained with a yield of 100%. ^{1}H-NMR ($CDCl_3$, 400 MHz) δ: 1.44 (t, 12 H, $J = 7.0$), 1.60 (d, 12 H, $J = 7.2$), 4.12–4.22 (m, 8H), 4.44 (q, 4 H, $J = 7.2$), 4.66 (q, 8 H, $J = 7.0$). The peak shifts were consistent with the structure and suggested that the compound was pure.

The desired *1,2;3,4*-di-O-isopropylidene-6-O-acryloyl-α-D-galactopyranose (AIpGP) was obtained with a yield of 94%. ^{1}H-NMR ($CDCl_3$, 400 MHz) δ: 1.35 (s, 3H), 1.37 (s, 3H), 1.48 (s, 3H), 1.53 (s, 3H), 4.07–4.11(m, 1 H), 4.27–4.32 (m, 2 H), 4.35 (dd, 1 H, $J = 2.5$, 5.0), 4.41 (dd, 1 H, $J = 4.7$, 11.6), 4.65 (dd, 1 H, $J = 2.5$, 7.9), 5.56 (d, 1 H, $J = 5.0$), 5.85 (dd, 1 H, $J = 1.4$, 10.4), 6.19 (dd, 1 H, $J = 1.4$, 10.4), 6.46 (dd, 1 H, $J = 1.4$, 17.4). The peak shifts were consistent with the structure and suggested that the compound was pure.

3.2.2.2. Synthesis of multi-arm polymers. The ^{1}H-NMR of multi-arm poly-(1,2:3,4-di-O-isopropylidene-6-O-methacryloyl-α-D-galactopyranose) was determined. ^{1}H-NMR (D_2O, 400 MHz) δ: 1.29–2.05 (brs, 1 H), 2.17–2.74 (brs, 2 H), 3.45–4.17 (brs, 6H), 5.26 (brs, 1 H).

The ^{1}H-NMR of multi-arm poly-(6-O-methacryloyl-D-galactose) was determined. ^{1}H-NMR (D_2O, 400 MHz) δ: 1.29–2.05 (brs, 1 H), 2.17–2.74 (brs, 2 H), 3.45–4.17 (brs, 6H), 5.26 (brs, 1 H).

3.2.2.3. Synthesis of JS-K and its analogues. The desired Boc-Hydrazine compound was obtained as a white solid with a yield of 54%. ^{1}H-NMR ($CDCl_3$, 400 MHz): $\delta = 1.81$–1.87 (m, 1H), 1.95 (brs, 1H), 2.06–2.12 (m, 2H), 2.27–2.33 (m, 1H), 2.88 (dd, $J = 10.2$, 7.8 Hz, 1H), 3.55 (ddd, $J = 16.6$, 10.8, 5.9 Hz, 1H), 3.68–3.73(m, 1H), 3.85 (dt, $J = 8.0$, 3.6 Hz, 1H), 4.23–4.25 (m, 1H), 7.16 (d, $J = 9.6$ Hz, 1H). 8.17 (dd, $J = 9.6$, 2.7 Hz, 1H), 8.66 (d, $J = 2.7$ Hz, 1H). The data was consistent with that reported previously.

The desired compound 1 was obtained as a yellow solid with a yield of 53%. ^{1}H-NMR ($CDCl_3$, 400 MHz): $\delta = 1.81$–1.87 (m, 1H), 1.95 (brs, 1H), 2.06–2.12 (m, 2H), 2.27–2.33 (m, 1H), 2.88 (dd, $J = 10.2$, 7.8 Hz, 1H), 3.55 (ddd, $J = 16.6$, 10.8, 5.9 Hz, 1H), 3.68–3.73(m, 1H), 3.85 (dt, $J = 8.0$, 3.6 Hz, 1H), 4.23–4.25 (m, 1H), 7.16 (d, $J = 9.6$ Hz, 1H). 8.17 (dd, $J = 9.6$, 2.7 Hz, 1H), 8.66 (d, $J = 2.7$ Hz, 1H). The data were consistent with that reported previously.

The desired compound 2 was obtained as a yellow solid with a yield of 96%. ^{1}H-NMR (DMSO-d_6, 400 MHz): $\delta = 3.35$ (brs, 4 H), 3.92 (brs, 4H), 7.98 (d, $J = 9.3$ Hz, 1H), 8.58 (dd, $J = 9.3$ Hz, 2.7 Hz, 1H), 8.89 (d, $J = 2.4$ Hz, 1H), 9.64 (brs, 2H). ^{13}C-NMR (DMSO-d_6, 100 MHz): $\delta = 41.8$, 47.4, 118.8, 122.3, 130.2, 137.4, 142.8, 153.0. HRMS (ESI) calculated for $C_{10}H_{13}N_6O_6$ $(M + H)^+$: 313.0897; Found: 313.0895.

The desired compound 3 was obtained as a yellow solid with a yield of 90%. ^{1}H-NMR ($CDCl_3$, 400 MHz): $\delta = 1.30$ (t, $J = 5.7$ Hz, 3H), 3.29 (brs, 4 H), 3.71 (t, $J = 5.2$ Hz, 4H), 4.20 (q, $J = 14.2$, 7.1 Hz, 2H), 7.14 (d, $J = 9.3$ Hz, 1H). 8.31 (dd, $J = 9.2$ Hz, 2.7 Hz, 1H), 8.90 (d, $J = 2.7$ Hz, 1H); ^{13}C-NMR ($CDCl_3$, 100 MHz): $\delta = 14.6$, 42.2, 50.5, 62.1, 117.7, 122.2, 129.1, 137.3, 142.4, 153.7, 155.0. HRMS (ESI) calculated for $C_{13}H_{16}N_6O_8$ $(M + Na)^+$: 407.0927; Found: 407.0932.

The desired compound 4 was obtained as a yellow solid with a yield of 64%. ^{1}H-NMR ($CDCl_3$, 400 MHz): $\delta = 2.42$ (brs, 1H), 2.66 (t, $J = 5.2$ Hz, 2H), 2.78 (t, $J = 4.9$ Hz, 4H), 3.68–3.73 (m, 6H), 7.69 (d, $J = 9.3$ Hz, 1H). 8.48 (dd, $J = 9.2$, 2.5 Hz, 1H), 8.89 (d, $J = 2.5$ Hz, 1H); ^{13}C-NMR ($CDCl_3$, 100 MHz): $\delta = 50.6$, 51.2, 58.1, 58.7, 117.6, 122.2, 129.1, 137.4, 142.7, 153.9. HRMS (ESI) calculated for $C_{12}H_{17}N_6O_7$ $(M + H)^+$: 357.1159; Found: 357.1144.

The desired compound 5 was obtained as a yellow solid with a yield of 68%. ^{1}H-NMR ($CDCl_3$, 400 MHz): $\delta = 1.69$ (brs, 1H), 2.70 (t, $J = 5.3$ Hz, 2H), 2.80 (t, $J = 5.1$ Hz, 4H), 3.63–3.66 (m, 2H), 3.69–3.75

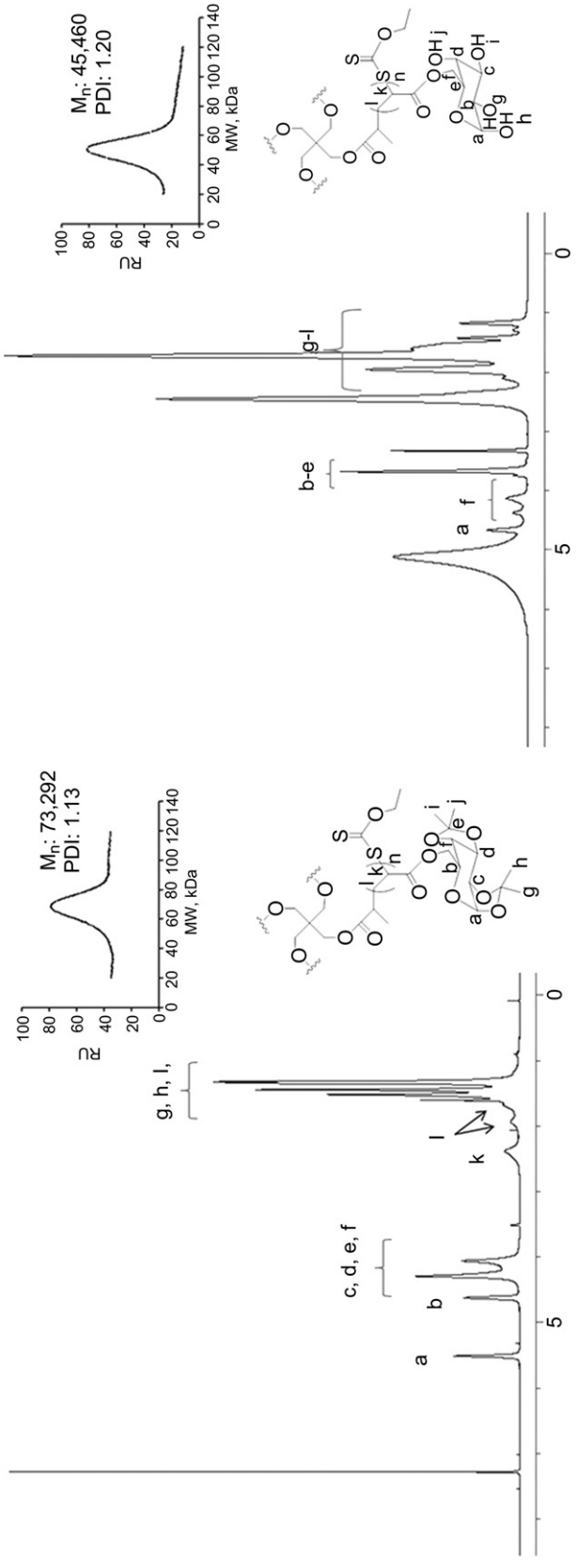

Fig. 7. (A) ^{1}H NMR spectra and (B) GPC traces of multi-arm poly-(1,2:3,4-*di*-*O*-isopropylidene-6-*O*-methacryloyl-α-D-galactopyranose) (M_n = 73,292 Da, PDI = 1.13) and multi-arm poly-(6-*O*-methacryloyl-D-galactose)) (M_n = 45,460 Da, PDI = 1.20).

(m, 8H), 7.68 (d, J = 9.3 Hz, 1H). 8.47 (dd, J = 9.2, 2.7 Hz, 1H), 8.90 (d, J = 2.7 Hz, 1H); ^{13}C-NMR ($CDCl_3$, 100 MHz): δ = 50.3, 51.5, 57.0, 61.9, 68.0, 72.3, 117.6, 122.2, 129.1, 137.2, 142.3, 153.9. HRMS (ESI) calculated for $C_{14}H_{21}N_6O_8$ $(M + H)^+$: 401.1421; Found: 401.1413.

3.2.2.4. Synthesis of multi-arm polymer-NO conjugate. The desired multi-arm poly-(6-O-methacryloyl-D-galactose)-acid-NO1 conjugate was obtained as a yellow solid with a yield of 29%. ^{1}H-NMR ($CDCl_3$, 400 MHz): δ = 1.81–1.87 (m, 1H), 1.95 (brs, 1H), 2.06–2.12 (m, 2H), 2.27–2.33 (m, 1H), 2.88 (dd, J = 10.2, 7.8 Hz, 1H), 3.55 (ddd, J = 16.6, 10.8, 5.9 Hz, 1H), 3.68–3.73(m, 1H), 3.85 (dt, J = 8.0, 3.6 Hz, 1H), 4.23–4.25 (m, 1H), 7.16 (d, J = 9.6 Hz, 1H). 8.17 (dd, J = 9.6, 2.7 Hz, 1H), 8.66 (d, J = 2.7 Hz, 1H).

3.2.3. Solubility

The solubilities of sugar polymer poly-(6-*O*-methacryloyl-D-galactose) and its acid-modified derivatives were determined in pH 7.4 PBS at 37 °C. The solubilities of sugar star polymer with 0, 20, 40, 60 and 90% acid substitution were determined to be 250, 273, 295, 314, and 309 mg/mL, respectively. The result suggested a linear increase in the solubility with increasing degrees of acid substitution from 0 to 60% wt (R^2 = 0.998). In addition, the intrinsic solubility of the polymer with 90% acid substitution did not further increase and it appeared to exhibit a similar solubility as the polymer with 60% acid substitution.

3.2.4. Viscosity

The viscosities of sugar multi-arm polymer, poly-(6-*O*-methacryloyl-D-galactose), and its acid-modified derivatives (sugar polymers with 20%, 40%, 60% and 90% acid substitution) were determined in ddH_2O at three increasing concentrations (1.0, 3.0 and 10.0 mg/mL) (Table 1). The polymers demonstrated low viscosities, merely 5–10% higher than pure H_2O, regardless of the percent of the acid substitution. Furthermore, the viscosities of various polymers with different degrees of acid substitution appeared to increase with increasing polymer concentrations from 1.0 to 10.0 mg/mL.

3.3. In vitro cytotoxicity

The cytotoxicity of nitric oxide-releasing prodrugs and polymer-based conjugates was determined in a human head and neck cancer cell line, MDA-1986, and human breast cancer cell lines, MDA-MB-468 and MDA-MB-231. The IC_{50} values of NO1, NO2, JS-K and sugar-NO1 are reported in Table 2. Prodrugs NO1 and NO2 had similar activity in all of the cell lines. The parent drug JS-K was more active than the prodrugs in MDA-1986 cells and less active in MDA-MB-468 cells. The sugar polymer-based conjugate was 1.6–5.3-fold less cytotoxic (mean of 2.5 fold) than the free prodrugs and JS-K in the tested cell lines.

3.4. Nitric oxide release in vitro

The release kinetics of nitric oxide prodrugs were determined in cell culture (DMEM with 10% bovine serum albumin and 1% L-glutamine) using human HNSCC cell line, MDA-1986. The concentration of nitrite, the stable breakdown product of gaseous nitric oxide, was measured using Griess assay as an indirect measurement of nitric oxide concentration in cell culture media. The assay is based on the reaction between sulfanilamide, *N*-1-napthyethylenediamine dihydrochloride and nitrite, under acidic conditions to produce a fluorescent azo compound. The half-life was determined by fitting the release data to a first order decay model using GraphPad 5 ($R^2 > 0.96$ for all fits). A nitrite calibration curve (R^2 = 0.99) was generated under the same condition using

Table 2
IC_{50} values and release half-lives of NO prodrugs (NO1, NO2 and JS-K) and multi-arm polymer-NO1 conjugates.

Prodrugs/conjugates	IC_{50}: MDA-1986	IC_{50}: MDA-MB-468	IC_{50}: MDA-MB-231	Release half-life, h
NO1	33 ± 1 μM	26 ± 4 μM	32 ± 3 μM	7.1
NO2	57 ± 6 μM	27 ± 3 μM	–	9.0
JS-K	16 ± 2 μM	42 ± 4 μM	–	3.2
Sugar-NO1	86 ± 9 μM	67 ± 6 μM	120 ± 14 μM	9.2

a series of nitrite solutions (0, 1.56, 3.13, 6.25, 12.5, 25, 50, and 100 μM).

All three nitric oxide prodrugs, NO1, NO2 and JS-K, as well as the sugar-NO1 conjugate, produced nitric oxide in a sustained manner, with generation half-lives of 7.1, 9.0, 3.2 and 9.2 h, respectively (Table 2, Fig. 8).

3.5. Treatment

We have established an orthotopic rodent xenograft model of human HNSCC with rapid and sustained tumor growth in our previous study [19]. Animals in either the control group or the JS-K i.v. treatment group had tumors with a size of approximately 1000 mm^3, five or six weeks after tumor cell implantation, respectively (Fig. 9A). In comparison, the animals treated with sugar-NO1 developed a tumor of an average size of approximately 200 mm^3 within the same time frame, which is 5-fold smaller than the tumor sizes observed in the control and JS-K i.v. groups. Additionally, 32.7% of animals in the sugar-NO1 group survived the study (21 weeks post-tumor cell injection), and two mice had a complete response (defined as no evidence of residual disease) within 14 weeks (Fig. 9A). On the contrary, 100% of the control or JS-K treated animals were euthanized within seven weeks either due to the tumor size exceeding 1000 mm^3 or necrosis of the injection site on the tail. Further, HNSCC tumor progression was delayed by nearly six weeks on average after s.c. sugar-NO1 therapy, and the survival rate was significantly extended relative to the control group ($\rho < 0.001$, Fig. 9B). The disease condition of each individual animal in the control or treated groups is reported in Table 3.

4. Discussion

Xanthate-mediated living radical polymerization using an MADIX/RAFT agent has been proven to successfully synthesize a number of polymeric materials, including star-shaped polymers [30] and functional diblocks [34], which could be introduced into the fields of chemical and pharmaceutical industries as additives, emulsifiers, surface coating materials as well as potential drug delivery vehicles.

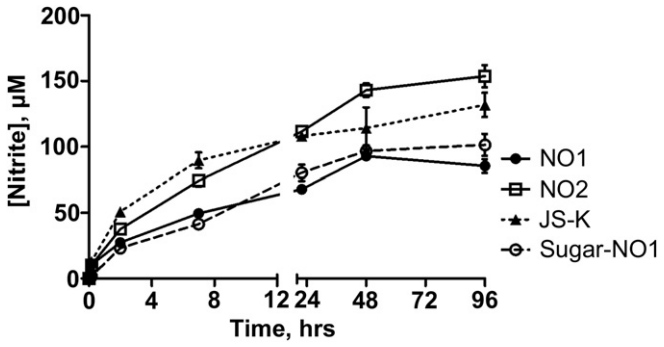

Fig. 8. In vitro production of nitric oxide by NO1, NO2, JS-K, and sugar-NO1 (20 μM starting concentration on NO basis). The release studies were conducted in DMEM in the presence of MDA-1986 cells. The release half-lives were determined to be 7.1, 9.0, 3.2 and 9.2 h, for NO1, NO2, JS-K and sugar-NO1, respectively.

In this study, we successfully synthesized a 4-arm branched polymer grafted with sugar moieties. The spherical multi-arm polymer has a compact structure, low polydispersity index and large surface area, making it an ideal candidate for drug delivery applications. In addition, the presence of a number of sugar molecules on the polymer chains effectively converts a hydrophobic synthetic polymer into a highly water-soluble and non-toxic polymer due to the ease of degradation of the sugar braches by the naturally-occurring enzymes in vivo. Although the polystyrene backbone is not biodegradable, the arms are connected to the core via esters subject to hydrolytic decomposition in vivo. The liberated polystyrene arms are below the renal exclusion limit and should clear from the systemic circulation. These unique properties of the polymer may be advantageous because they could be readily translated into practical benefits, including: the elimination of the presence of any organic solvents in its aqueous solution; the satisfactory injectability of even the highly concentrated polymer solution due to its low viscosity similar to water; and the low toxicity compared to other synthetic polymers, such as PAMAM dendrimers, due to its biodegradability and low cytotoxicity.

The intrinsic solubilities of the acid multi-arm polymers was highly correlated with increasing degrees of acid substitution ($R^2 = 0.998$). As the degree of acid substitution increased (0, 20, 40 and 60%), the surface charge density of the polymers as well as the average number of hydrogen bonds between the carboxylic acid groups of the polymer and the water molecules also increased, leading to favorable enthalpic interactions between the polymer and the surrounding water molecules along with the desired intra- and inter-molecular electrostatic repulsions within the multi-arm polymer itself [35,36]. The linear solubility characteristic of the acid multi-arm polymers could be further applied to other natural, semi-synthetic or synthetic polymers, promoting and possibly predicting the solubilities of their acid-modified derivatives. As the degree of acid substitution increased beyond 60%, the solubility of the resulting acid polymers plateaued and did not further increase. It is likely due to the possible crosslinking between the highly abundant carboxylic acid groups and the hydroxyl groups of the sugar molecules, reducing the flexibility of the polymer chains and restricting the overall dynamics of the polymer structure.

Low viscosity is crucial for local injectables, since injection volumes are much smaller than intravenous treatments and smaller bore needles are desired for patient comfort. High viscosity is usually associated with low injectability and great discomfort at the injection site. The sugar multi-arm polymer our laboratory synthesized demonstrated extremely low intrinsic viscosity at 1% w/v compared to other polymers for local injection, such as hyaluronan [37], resulting in a smooth delivery of high doses of therapeutics via a relatively small volume of injection.

In addition to the synthesis of this multi-arm polymer nanocarrier, the synthesis, characterization and in vivo effectiveness of two nitric-oxide releasing prodrugs, NO1 and NO2, are also reported. Since the emergence of JS-K, a glutathione s-transferase (GST)-activated nitric oxide prodrug, the underlying mechanisms regulating nitric oxide-induced cell death have been extensively investigated. To date, multiple signaling pathways have been discovered to be involved in promoting the death of cancer cells, suggesting NO is likely to mediate cell proliferation via multiple complex pathways. Sang et al. proposed that nitric oxide donating prodrugs may trigger the apoptosis of gastric cancer cells via the inactivation of AKT, a serine/threonine protein kinase, resulting in the dysregulation of cell cycle-associated proteins, and thus leading to G0/G1 arrest and the corresponding cell growth inhibition [38]. According to a study conducted by Mijatovic et al., nitric oxide also

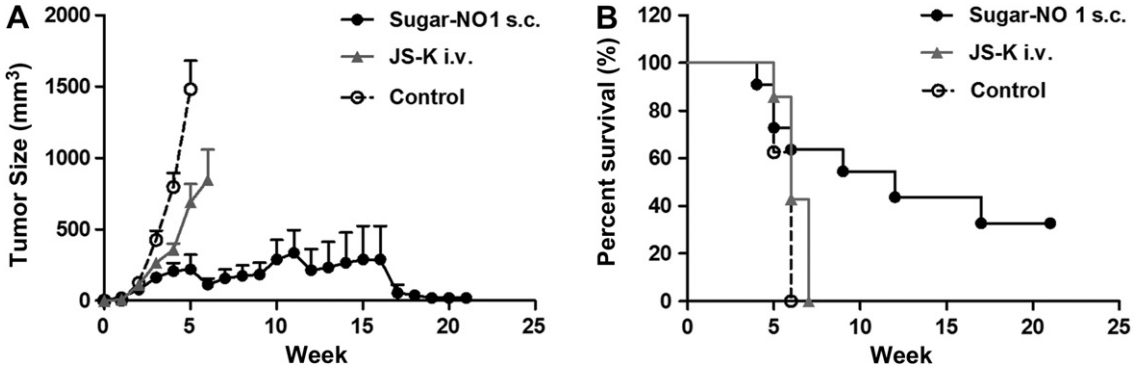

Fig. 9. A) Size measurements of head and neck tumors and B) survival rates of the animals. Treatment groups include: Sugar-NO1 (10 mg/kg dose on NO1 basis, s.c., $N = 11$), JS-K (10 mg/kg dose, i.v., $N = 7$) and treatment-free control ($N = 8$). Errors were reported in standard error of the mean.

can induce apoptosis of melanoma cells via a TRAIL-mediated pathway, in which cells are sensitized to TRAIL and the expression of inducible nitric oxide synthase (iNOS) is altered [39]. Furthermore, Kim et al. demonstrated that nitric oxide-induced apoptosis of colon cancer cells is associated with caspases activation and it may be attributed to the downregulation of the anti-apoptotic Bcl-2 oncoprotein, along with the activation of p53 signaling pathway [40].

Due to the complex nature of NO mediated cell death, it is less likely for cancer cells to develop a series of acquired resistance mechanisms against all governing pathways. Therefore, we sought to design a long-acting, nitric oxide-donating nanocarrier that could be given as locoregional chemotherapy for locally advanced cancers, including head and neck cancer and breast cancer, to generate cytotoxic nitric oxide molecules over time in a sustained pattern. The in vitro nitric oxide release data elucidated that the synthesized nitric oxide prodrugs, NO1 and NO2, both demonstrated longer nitric oxide release half lives in head and neck cancer cells. Additionally, the sugar-NO1 nanoconjugate exhibited the longest release half-life, which was 2.9-fold longer than the model NO-releasing drug, JS-K. The longer half-lives of the prodrugs compared to JS-K are due to the presence of electron-donating groups on the nitrogen of the 6-membered ring, which resists nucleophilic attack and generation of the Meisenheimer intermediate, whereas the carboxy in JS-K is electron-withdrawing. In addition, the sugar-NO1 conjugate may have extended the half-life by sterically hindering the prodrug from nucleophilic attack by reactive thiols. Therefore, if the in vitro drug release kinetics correctly represents the in vivo conditions, the sugar-NO1 conjugate may be a promising candidate for the controlled release of nitric oxide in tumor-bearing animals. According to a study conducted by Azizzadeh et al., NO-producing prodrugs with a longer release half-life may be more potent inhibitors of DNA synthesis and mitotic activity in the S-phase compared to short-lived NO-prodrugs [41].

Table 3
Disease condition of tumor-bearing mice in control, i.v. JS-K and s.c. Sugar-NO1 treatment groups. Tumor response was reported based on modified RECIST criteria. CR = Complete response (no gross evidence of tumor); PR = Partial response (>30% reduction); SD = Stable disease (neither PR nor PD criteria met); PD = Progressive disease (>30% tumor growth). Mice with an ulcerated tumor that were euthanized before the end of the study were excluded from this analysis.

Treatment group	No.1	No.2	No.3	No.4	No.5	No.6	No.7	No.8
Sugar NO1 s.c.	PR	PD	CR	PD	PD	PR	CR	SD
JS-K i.v.	PD	Necrosis	PD	PD	Necrosis	PD	–	–
Control	PD	PD	PD	PD	PD	PD	PD	–

Compared to JS-K, both unbound NO1 and NO2 had slightly higher IC_{50} values in MDA-1986 cells, whereas, they both showed higher in vitro toxicity in MDA-MB-468 cells. Even though the carrier-based sugar-NO1 conjugate had higher IC_{50} values than the standard JS-K, according to our previous studies using hyaluronan-cisplatin and hyaluronan-doxorubicin conjugates, the subcutaneously administered, sustained nitric oxide-releasing platform may provide additional benefits including: modified drug pharmacokinetics by avoiding the potentially harmful C_{max}; reduced systemic toxicities due to limited drug exposure within the circulatory system and highly perfused, toxin-susceptible organs (kidneys, liver and heart); and improved local disease control via localized delivery of highly concentrated NO therapy [18–22].

In the following in vivo evaluation of the anti-cancer efficacy of the sugar-NO1 therapy, we demonstrated that the subcutaneously injected conjugate (10 mg/kg) significantly improved the tumor inhibition in HNSCC xenografts, extending the average life span of the animals by six weeks, which was approximately one third the length of the time frame of the study. In contrast, the intravenous therapy of JS-K at an equivalent dose only resulted in a slight regression of tumor growth and a very limited increase of animals average survival rate. In addition, the localized injection also provided benefit in terms of tumor response, compared to the i.v. therapy, resulting in 25% of complete response and 25% of partial response. Unfortunately the entire group of animals received i.v. therapy developed progressive disease and none of them responded to the JS-K treatment. Furthermore, one third of the animals in the JS-K i.v. group experienced necrosis and inflammation of the injection site on their tails, which may be attributed to the toxicity of JS-K.

Besides HNSCC, this localized drug delivery platform could be adapted to other types of cancers, including breast cancer and prostate cancer, which were shown to be responsive to JS-K therapy [12,13,42,43]. Furthermore, recent investigations have discovered that nitric oxide may be involved in the reversal of cisplatin resistance in head and neck cancer [44], ovarian cancer [45,46] and lung cancer [47], via mechanisms of survivin modulation, depletion of cellular thiols, and inhibition of Bcl-2 ubiquitination, respectively. Similar re-sensitizing effects of nitric oxide were also reported in the reversal of doxorubicin chemo-resistance in human colon cancer [48]. Herein, this NO-eluting nanocarrier could either be utilized as a single treatment for JS-K responsive cancers, or incorporated into a combination therapy regimen to revert drug-induced chemo-resistance. Our ongoing studies will focus on optimizing the in vitro and in vivo properties of this type of nitric oxide-releasing nanocarriers, laying the foundation for future translational study, to develop a safe and effective nitric oxide formulation for treating cisplatin and doxorubicin resistant cancers.

5. Conclusions

We have developed a locoregional nitric oxide delivery platform for treating locally advanced head and neck cancer using multi-arm polymer nanocarriers. The polymeric architectures were successfully synthesized and characterized, which released nitric oxide chemotherapy in a sustained fashion, and significantly inhibited the growth of HNSCC in vivo.

Acknowledgments

This work was supported by awards from the National Institutes of Health (R21 CA132033 and P20 RR016475), the American Cancer Society (RSG-08-133-01-CDD), and the Susan G. Komen Foundation (KG 090481).

References

[1] Vokes EE, Weichselbaum RR, Lippman SM, Hong WK. Head and neck cancer. N Engl J Med 1993;328:184–94.
[2] Wilken R, Veena MS, Wang MB, Srivatsan ES. Curcumin: a review of anti-cancer properties and therapeutic activity in head and neck squamous cell carcinoma. Mol Cancer 2011;10:12.
[3] Singh S, Gupta AK. Nitric oxide: role in tumour biology and iNOS/NO-based anticancer therapies. Cancer Chemother Pharmacol 2011;67:1211–24.
[4] Abdelmagid SA, Too CK. Prolactin and estrogen up-regulate carboxypeptidase-d to promote nitric oxide production and survival of mcf-7 breast cancer cells. Endocrinology 2008;149:4821–8.
[5] Clementi E, Nisoli E. Nitric oxide and mitochondrial biogenesis: a key to long-term regulation of cellular metabolism. Comp Biochem Physiol A Mol Integr Physiol 2005;142:102–10.
[6] Donia M, Maksimovic-Ivanic D, Mijatovic S, Mojic M, Miljkovic D, Timotijevic G, et al. In vitro and in vivo anticancer action of Saquinavir-NO, a novel nitric oxide-derivative of the protease inhibitor saquinavir, on hormone resistant prostate cancer cells. Cell Cycle 2011;10:492–9.
[7] Huerta-Yepez S, Vega M, Jazirehi A, Garban H, Hongo F, Cheng G, et al. Nitric oxide sensitizes prostate carcinoma cell lines to TRAIL-mediated apoptosis via inactivation of NF-kappa B and inhibition of Bcl-xl expression. Oncogene 2004;23:4993–5003.
[8] Stewart GD, Nanda J, Katz E, Bowman KJ, Christie JG, Brown DJ, et al. DNA strand breaks and hypoxia response inhibition mediate the radiosensitisation effect of nitric oxide donors on prostate cancer under varying oxygen conditions. Biochem Pharmacol 2011;81:203–10.
[9] Royle JS, Ross JA, Ansell I, Bollina P, Tulloch DN, Habib FK. Nitric oxide donating nonsteroidal anti-inflammatory drugs induce apoptosis in human prostate cancer cell systems and human prostatic stroma via caspase-3. J Urol 2004;172:338–44.
[10] Baritaki S, Huerta-Yepez S, Sahakyan A, Karagiannides I, Bakirtzi K, Jazirehi A, et al. Mechanisms of nitric oxide-mediated inhibition of EMT in cancer: inhibition of the metastasis-inducer snail and induction of the metastasis-suppressor RKIP. Cell Cycle 2010;9:4931–40.
[11] Cooper CE. Nitric oxide and iron proteins. Biochim Biophys Acta 1999;1411: 290–309.
[12] Shami PJ, Saavedra JE, Wang LY, Bonifant CL, Diwan BA, Singh SV, et al. JS-K, a glutathione/glutathione S-transferase-activated nitric oxide donor of the diazeniumdiolate class with potent antineoplastic activity. Mol Cancer Ther 2003;2:409–17.
[13] McMurtry V, Saavedra JE, Nieves-Alicea R, Simeone AM, Keefer LK, Tari AM. JS-K, a nitric oxide-releasing prodrug, induces breast cancer cell death while sparing normal mammary epithelial cells. Int J Oncol 2011;38: 963–71.
[14] Maciag AE, Chakrapani H, Saavedra JE, Morris NL, Holland RJ, Kosak KM, et al. The nitric oxide prodrug JS-K is effective against non-small-cell lung cancer cells in vitro and in vivo: involvement of reactive oxygen species. J Pharmacol Exp Ther 2011;336:313–20.
[15] Kiziltepe T, Hideshima T, Ishitsuka K, Ocio EM, Raje N, Catley L, et al. JS-K, a GST-activated nitric oxide generator, induces DNA double-strand breaks, activates DNA damage response pathways, and induces apoptosis in vitro and in vivo in human multiple myeloma cells. Blood 2007;110:709–18.
[16] Boyer TD. The glutathione S-transferases: an update. Hepatology 1989;9: 486–96.
[17] Swarts JC, Swarts DM, Maree DM, Neuse EW, La Madeleine C, Van Lier JE. Polyaspartamides as water-soluble drug carriers. part 1: antineoplastic activity of ferrocene-containing polyaspartamide conjugates. Anticancer Res 2001;21:2033–7.
[18] Cai S, Thati S, Bagby TR, Diab HM, Davies NM, Cohen MS, et al. Localized doxorubicin chemotherapy with a biopolymeric nanocarrier improves survival and reduces toxicity in xenografts of human breast cancer. J Control Release 2010;146:212–8.
[19] Cai S, Xie Y, Davies NM, Cohen MS, Forrest ML. Carrier-based intralymphatic cisplatin chemotherapy for the treatment of metastatic squamous cell carcinoma of the head & neck. Ther Deliv 2010;1:237–45.
[20] Cai S, Xie Y, Davies NM, Cohen MS, Forrest ML. Pharmacokinetics and disposition of a localized lymphatic polymeric hyaluronan conjugate of cisplatin in rodents. J Pharm Sci 2010;99:2664–71.
[21] Cai S, Xie Y, Bagby TR, Cohen MS, Forrest ML. Intralymphatic chemotherapy using a hyaluronan-cisplatin conjugate. J Surg Res 2008;147:247–52.
[22] Cohen MS, Cai S, Xie Y, Forrest ML. A novel intralymphatic nanocarrier delivery system for cisplatin therapy in breast cancer with improved tumor efficacy and lower systemic toxicity in vivo. Am J Surg 2009;198: 781–6.
[23] Inoue S, Ding H, Portilla-Arias J, Hu J, Konda B, Fujita M, et al. Polymalic acid-based nanobiopolymer provides efficient systemic breast cancer treatment by inhibiting both HER2/neu receptor synthesis and activity. Cancer Res 2011;71: 1454–64.
[24] Eldar-Boock A, Miller K, Sanchis J, Lupu R, Vicent MJ, Satchi-Fainaro R. Integrin-assisted drug delivery of nano-scaled polymer therapeutics bearing paclitaxel. Biomaterials 2011;32:3862–74.
[25] Xie Y, Aillon KL, Cai S, Christian JM, Davies NM, Berkland CJ, et al. Pulmonary delivery of cisplatin-hyaluronan conjugates via endotracheal instillation for the treatment of lung cancer. Int J Pharm 2010;392:156–63.
[26] Daftarian P, Kaifer AE, Li W, Blomberg BB, Frasca D, Roth F, et al. Peptide-conjugated PAMAM dendrimer as a universal DNA vaccine platform to target antigen-presenting cells. Cancer Res 2011;71:7452–62.
[27] Bai S, Ahsan F. Synthesis and evaluation of pegylated dendrimeric nanocarrier for pulmonary delivery of low molecular weight heparin. Pharm Res 2009;26: 539–48.
[28] Talanov VS, Regino CA, Kobayashi H, Bernardo M, Choyke PL, Brechbiel MW. Dendrimer-based nanoprobe for dual modality magnetic resonance and fluorescence imaging. Nano Lett 2006;6:1459–63.
[29] Kobayashi H, Kawamoto S, Bernardo M, Brechbiel MW, Knopp MV, Choyke PL. Delivery of gadolinium-labeled nanoparticles to the sentinel lymph node: comparison of the sentinel node visualization and estimations of intra-nodal gadolinium concentration by the magnetic resonance imaging. J Control Release 2006;111:343–51.
[30] Stenzel MH, Davis TP, Barner-Kowollik C. Poly(vinyl alcohol) star polymers prepared via MADIX/RAFT polymerisation. Chem Commun (Camb); 2004:1546–7.
[31] Ting SR, Gregory AM, Stenzel MH. Polygalactose containing nanocages: the RAFT process for the synthesis of hollow sugar balls. Biomacromolecules 2009;10:342–52.
[32] Chakrapani H, Goodblatt MM, Udupi V, Malaviya S, Shami PJ, Keefer LK, et al. Synthesis and in vitro anti-leukemic activity of structural analogues of JS-K, an anti-cancer lead compound. Bioorg Med Chem Lett 2008;18:950–3.
[33] Ullman-Cullere MH, Foltz CJ. Body condition scoring: a rapid and accurate method for assessing health status in mice. Lab Anim Sci 1999;49:319–23.
[34] Destarac M, Guinaudeau A, Geagea R, Mazieres S, Van Gramberen E, Boutin C, et al. Aqueous MADIX/RAFT polymerization of diallyldimethylammonium chloride: extension to the synthesis of poly(DADMAC)-based double hydrophilic block copolymers. J Polym Sci Part A Polym Chem 2010;48:5163–71.
[35] Gong P, Genzer J, Szleifer I. Phase behavior and charge regulation of weak polyelectrolyte grafted layers. Phys Rev Lett 2007;98:018302.
[36] Kuroda K, Swager TM. Synthesis of a nonionic water soluble semiconductive polymer. Chem Commun (Camb); 2003:26–7.
[37] Elder AN, Dangelo NM, Kim SC, Washburn NR. Conjugation of beta-sheet peptides to modify the rheological properties of hyaluronic acid. Biomacromolecules 2011;12:2610–6.
[38] Sang J, Chen Y, Tao Y. Nitric oxide inhibits gastric cancer cell growth through the modulation of the Akt pathway. Mol Med Rep 2011;4:1163–7.
[39] Mijatovic S, Maksimovic-Ivanic D, Mojic M, Timotijevic G, Miljkovic D, Mangano K, et al. Cytotoxic and immune-sensitizing properties of nitric oxide-modified Saquinavir in iNOS-positive human melanoma cells. J Cell Physiol 2011;226:1803–12.
[40] Kim MY, Trudel LJ, Wogan GN. Apoptosis induced by capsaicin and resveratrol in colon carcinoma cells requires nitric oxide production and caspase activation. Anticancer Res 2009;29:3733–40.
[41] Azizzadeh B, Yip HT, Blackwell KE, Horvath S, Calcaterra TC, Buga GM, et al. Nitric oxide improves cisplatin cytotoxicity in head and neck squamous cell carcinoma. Laryngoscope 2001;111:1896–900.
[42] Simeone AM, McMurtry V, Nieves-Alicea R, Saavedra JE, Keefer LK, Johnson MM, et al. TIMP-2 mediates the anti-invasive effects of the nitric oxide-releasing prodrug JS-K in breast cancer cells. Breast Cancer Res 2008; 10:R44.
[43] Shami PJ, Saavedra JE, Bonifant CL, Chu J, Udupi V, Malaviya S, et al. Antitumor activity of JS-K [O2-(2,4-dinitrophenyl) 1-[(4-ethoxycarbonyl)piperazin-1-yl] diazen-1-ium-1,2-diolate] and related O2-aryl diazeniumdiolates in vitro and in vivo. J Med Chem 2006;49:4356–66.
[44] Fetz V, Bier C, Habtemichael N, Schuon R, Schweitzer A, Kunkel M, et al. Inducible NO synthase confers chemoresistance in head and neck cancer by modulating survivin. Int J Cancer 2009;124:2033–41.
[45] Bratasz A, Selvendiran K, Wasowicz T, Bobko A, Khramtsov VV, Ignarro LJ, et al. NCX-4040, a nitric oxide-releasing aspirin, sensitizes drug-resistant human ovarian xenograft tumors to cisplatin by depletion of cellular thiols. J Transl Med 2008;6:9.

[46] Bratasz A, Weir NM, Parinandi NL, Zweier JL, Sridhar R, Ignarro LJ, et al. Reversal to cisplatin sensitivity in recurrent human ovarian cancer cells by NCX-4016, a nitro derivative of aspirin. Proc Natl Acad Sci U S A 2006;103:3914–9.
[47] Chanvorachote P, Nimmannit U, Stehlik C, Wang L, Jiang BH, Ongpipatanakul B, et al. Nitric oxide regulates cell sensitivity to cisplatin-induced apoptosis through S-nitrosylation and inhibition of Bcl-2 ubiquitination. Cancer Res 2006;66:6353–60.
[48] Riganti C, Miraglia E, Viarisio D, Costamagna C, Pescarmona G, Ghigo D, et al. Nitric oxide reverts the resistance to doxorubicin in human colon cancer cells by inhibiting the drug efflux. Cancer Res 2005;65:516–25.